

Content from this work may be used under the terms of the CC BY 3.0 licence (© 2018). Any distribution of this work must maintain attribution to the author(s), title of the work, publisher, and DOI.

# SIMULATIONS OF COHERENT ELECTRON COOLING WITH FREE ELECTRON LASER AMPLIFIER AND PLASMA-CASCADE MICRO-BUNCHING AMPLIFIER

J. Ma<sup>1</sup>, G. Wang<sup>1</sup>, V. N. Litvinenko<sup>1,2</sup>

<sup>1</sup> Brookhaven National Laboratory, Upton, New York 11973, USA

<sup>2</sup> Stony Brook University, Stony Brook, New York 11794, USA

## Abstract

SPACE is a parallel, relativistic 3D electromagnetic Particle-in-Cell (PIC) code used for simulations of beam dynamics and interactions. An electrostatic module has been developed with the implementation of Adaptive Particle-in-Cloud method. Simulations performed by SPACE are capable of various beam distribution, different types of boundary conditions and flexible beam line, as well as sufficient data processing routines for data analysis and visualization. Code SPACE has been used in the simulation studies of coherent electron cooling experiment based on two types of amplifiers, the free electron laser (FEL) amplifier and the plasma-cascade micro-bunching amplifier.

## COHERENT ELECTRON COOLING

Coherent electron cooling (CeC) [1, 2, 3] is a novel and promising technique for rapidly cooling high-intensity, high-energy hadron beams. A general CeC scheme consists of three sections: modulator, amplifier and kicker. In the modulator, the ion beam co-propagates with electron beam and each ion imprints a density wake on the electron distribution through Coulomb force. In the amplifier, the density modulation induced by ions is amplified by orders. In the kicker, the electron beam with amplified signal interacts with ion beam, giving coherent energy kick to ions towards their central energy, which consequently leads to cooling of the ion beam.

Figure 1 [3] shows the schematic of CeC using high gain free electron laser (FEL) as the amplifier, which is related with the CeC experiment in the Relativistic Heavy Ion Collider (RHIC) at the Brookhaven National Laboratory (BNL).

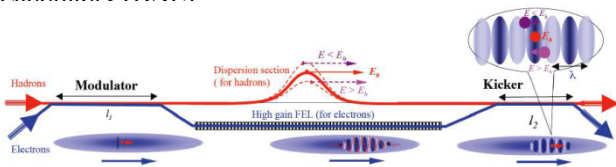


Figure 1: Schematic of coherent electron cooler based on high gain free electron laser.

Figure 2 [4] illustrates the layout of a CeC with a plasma-cascade amplifier (PCA). In the PCA, we use solenoids to control the transverse size of electron beam and make use of the exponential instability of longitudinal plasma oscillations to amplify the initial modulation. A CeC with a PCA does not require bending of ion beam.

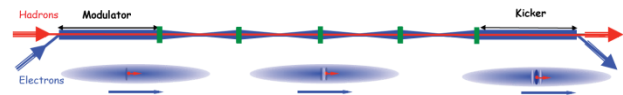


Figure 2: Layout of coherent electron cooler with a plasma-cascade amplifier.

## SIMULATION TOOL

Our main simulation tool is code SPACE [5]. SPACE is a parallel, relativistic, 3D electromagnetic Particle-in-Cell (PIC) code developed for the simulations of relativistic particle beams, beam-plasma interaction, and plasma chemistry. Benchmark test has been performed for SPACE with several accelerator physics codes including MAD-X, ELEGANT and Impact-T, and a good agreement has been achieved. SPACE has been used for the study of plasma dynamics in a dense gas filled RF cavity [6] and the study of mitigation effect by beam induced plasma [7].

Electrostatic module contained in code SPACE has been mainly used in our study, as the particle interaction is essentially electrostatic in the co-moving frame. This code module includes two different approaches. The first one is the traditional PIC method for the Poisson-Vlasov equation, which uses uniform Cartesian mesh, linear charge deposition scheme and fast Fourier transform (FFT) solver. This approach is precise and effective for particles with uniform distribution and computational domain with pure periodic boundary condition. The second approach is a new adaptive Particle-in-Cloud (AP-Cloud) method [8]. This method, based on real particle distribution, generates an adaptively chosen set of computational particles as the mesh, and uses the weighed least squares method for approximation of differential and integral operators. AP-Cloud method is beneficial for particles with non-uniform distribution and computational domain with irregular geometry and mixed type of boundary conditions, such as open boundary condition in the transverse directions and periodic in the longitudinal direction. Both approaches have passed series of verification tests and have been compared in our study. AP-Cloud method produced higher accuracy for electron beam with Gaussian distribution and computational domain with mixed boundary conditions, which are used in CeC simulations, so we have used AP-Cloud method in this study.

SPACE contains various data processing routines and provides sufficient output for data analysis and

visualization. The optional output files from code SPACE includes full 6-D particle distribution, integrated 3-D density distribution in given subset of the computational domain, projected 2-D density distribution on given plane, 1-D density and velocity distribution along longitudinal and transverse directions, particle distribution in phase space and frequency domain, beam parameters including transverse size and emittance.

GENESIS [9] is a three dimensional, time dependent code, developed for high gain FEL simulations. This code has been used in the simulations of FEL amplifier in our study.

## SIMULATIONS OF CEC WITH FEL AMPLIFIER

### *Algorithm and Verification*

In modulator, the first section of CeC, ions induce modulations in electron beam by attracting surrounding electrons. The relative modulation of electrons due to their interactions with ions is orders of magnitudes smaller than unity, therefore we can co-propagate a single ion with electron beam in modulator simulations and use super position principle to get the modulations by all ions. One of the difficulties using a single ion is the detection of the density and velocity modulation in electron beam, as the signal is too weak compared to the shot noise in electrons. The following algorithm has been used to extract the modulation signal induced by a single ion. We perform two simulations with identical initial distribution of electron, one simulation operates with electron beam only while the other simulation includes a single ion. At the exit of modulator, we can take difference in the electron distribution from the two simulations, to obtain the influence from the single ion. Figure 3 illustrates the typical signal-to-noise ratio in modulator simulations and clearly shows that the shot noise has been eliminated when we extract the modulation signal. Similar algorithm has been used in simulating the FEL amplification process with shot noise [10].

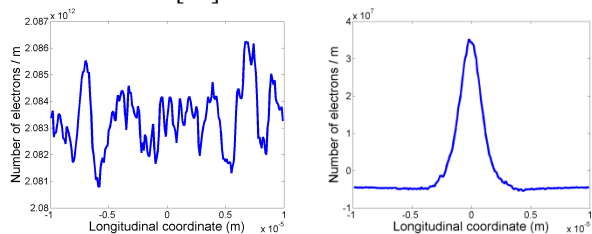


Figure 3: Comparison between shot noise in electrons (left) and modulation by a single ion (right) in longitudinal density distribution of electrons.

We have justified the super position principle in our simulations, as is shown in Figure 4. The blue solid line in Figure 4 shows the summation of density modulations by two ions from separate simulations, and the red dash line is the resulting density modulation when we put the two ions in the same run of simulation. These two modulation signals achieve a good agreement. Therefore, we can use

single ion in our simulations studies of CeC and follow super position principle to get the modulations induced by all ions in a beam.

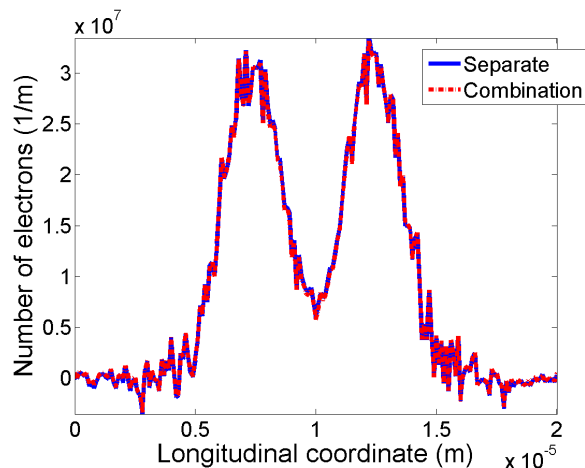


Figure 4: Comparison of density modulations induced by two ions from separate simulations (blue solid line) and from the same simulation (red dash line).

We have verified modulator simulation results through the comparison with theory. Analytical solution to the modulation problem exists for a moving ion co-propagating with an infinite electron beam with uniform spatial distribution [11]. Our simulation results have achieved a good agreement with the analytical solution [12], as is shown in Figure 5 [13].

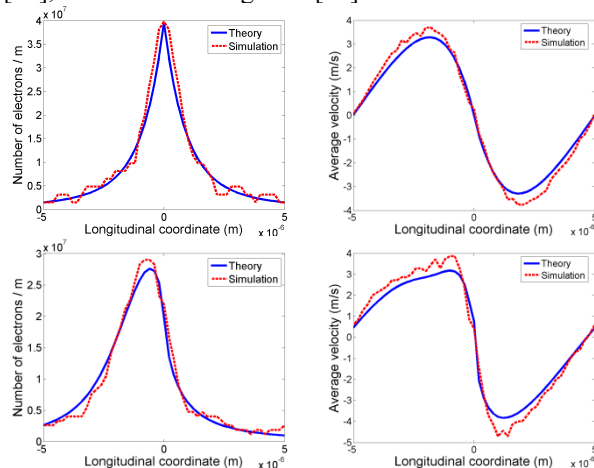


Figure 5: Comparison between theory and numerical simulations in density (left) and velocity (right) modulations by a single ion with reference energy (top) and off-reference energy (bottom) with respect to uniform electron cloud.

### *Modulator*

We list main parameters of electron and ion beams in Table 1. These parameters are related with the operations of CeC experiment at BNL RHIC, and have been used in numerical simulations to predict the cooling time.

Figure 6 shows the dynamics of  $\beta$  functions of electron beam in the modulator. Quadrupoles are used to focus the electrons in the beam line and to match the transverse beam size at the exit of modulator to obtain high gain in

Content from this work may be used under the terms of the CC BY 3.0 licence (© 2018). Any distribution of this work must maintain attribution to the author(s), title of the work, publisher, and DOI.

FEL amplifier, the second section of CeC. Electron beam dynamics in a quadrupole beam line using code SPACE have been benchmarked with other accelerator simulations tools, including MAD-X, ELEGANT and Impact-T [13, 14].

Table 1: Parameters of Electron and Ion Beams

	Electron	Ion, Au <sup>+79</sup>
Beam energy	$\gamma=28.5$	$\gamma=28.5$
Peak current	75 A	
Normalized emittance	$8 \pi$ mm mrad	$2 \pi$ mm mrad
R.M.S. energy spread	$1e-3$	$3e-4$

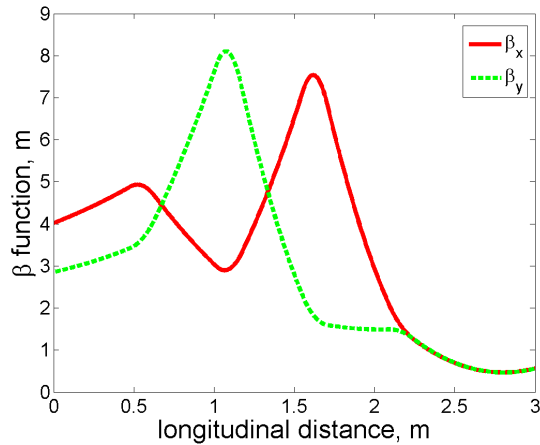


Figure 6: Evolution of electron beam  $\beta$  function in modulator section.

Figure 7 shows that the longitudinal density modulation gradually builds up when the ion co-propagates with the electron beam in modulator.

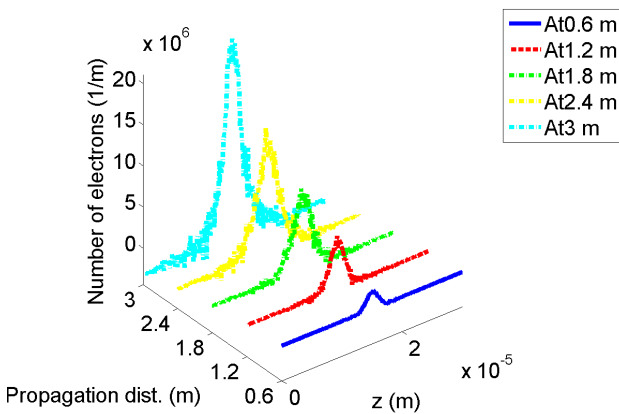


Figure 7: Longitudinal density modulation at several propagation distances in modulator.

We use the parameter bunching factor to quantify the longitudinal modulation. Bunching factor is also used in code GENESIS to obtain the gain in FEL simulations, and is defined in Equation (1) [9],

$$b \equiv \frac{1}{N_\lambda} \sum_{k=1}^{N_\lambda} e^{i \frac{2\pi}{\lambda_{opt}} z_k}, \quad -\frac{\lambda_{opt}}{2} \leq z_k \leq \frac{\lambda_{opt}}{2} \quad (1)$$

where  $\lambda_{opt}$  is the FEL optical wavelength, the summation is over a slice of  $\lambda_{opt}$  wide, centered at the ion's location, and  $N_\lambda$  is the total number of electrons within that slice.

The longitudinal density modulation shown in Figure 7 is induced by a single ion with reference energy and zero transverse offset with respect to the center of the electron beam, and is expected to achieve maximum bunching factor at the exit of modulator. Bunching factor reduces when we start with a single ion with transverse offsets. Figure 8 shows that the modulation becomes weaker when the ion is further away from the center of the electron beam in transverse plane. The dependence of bunching factor on transverse offsets is not symmetric in horizontal direction and vertical direction, as the transverse beam size is not symmetric in the quadrupole beam line, which is shown in Figure 6.

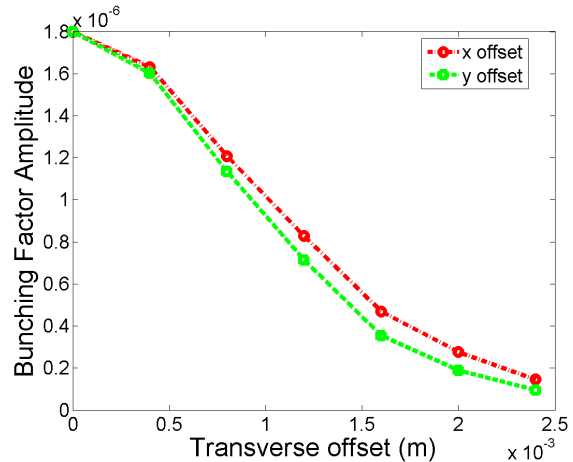


Figure 8: Amplitude of bunching factor induced by ions with various transverse offsets with respect to the center of the Gaussian electron beam.

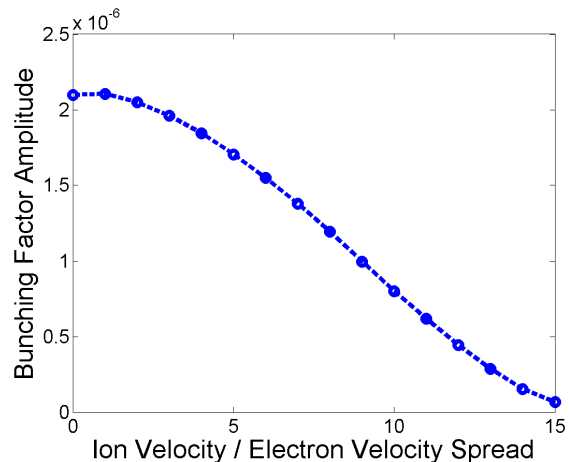


Figure 9: Amplitude of bunching factor induced by ions with various longitudinal velocities with respect to ions the electron beam group velocity. Ion velocity is in the unit of electrons' velocity spread.

Dependence of bunching factor on the energy difference between ions and electrons has also been studied [12], as is shown in Figure 9. Detailed studies have been performed to simulate the modulation process using ions with various combinations of off-reference energies, transverse offsets and transverse velocities [15].

### FEL Amplifier

We have exported the full 6-D particle distribution at the exit of modulator from code SPACE and imported it into code GENESIS to simulate the second section of CeC, FEL amplifier. GENESIS separate particles into longitudinal slices, and the length of each slice is FEL optical wavelength, which is about  $30 \mu\text{m}$  for our settings.

The FEL device installed at BNL RHIC has three sections of wigglers separated by drift space. It is difficult to achieve an envelope with constant transverse beam size over the three-section wigglers. Instead, we have designed an envelope with oscillating beam size and minimized the overall variation, which is shown in Figure 10.

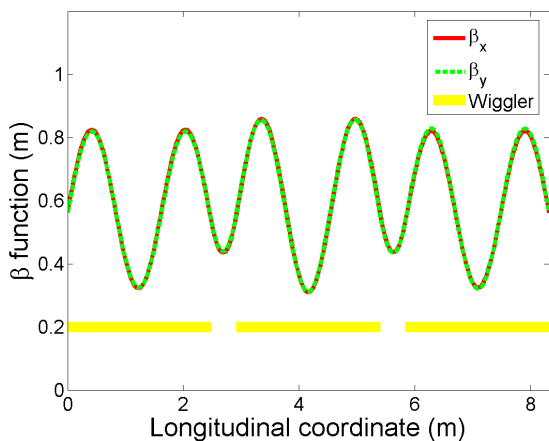


Figure 10: Location of three-section wigglers in FEL amplifier and  $\beta$  function evolution with minimum overall variation.

In FEL section, both the shot noise and the modulation signal are amplified. We need to maximum the gain from FEL to reduce the cooling time, and we should avoid saturation to preserve the correlation between the amplified signal and the ion which induces the initial modulation.

Figure 11 displays the growth of bunching factor of shot noise in FEL and shows that saturation is not reached at the end of FEL section. Figure 12 gives comparison of bunching factor between the initial density modulation at the entrance of FEL section and the final amplified signal at the exit of FEL. This signal has been extracted from the shot noise using the similar algorithm applied in modulator simulations. The comparison in Figure 12 clearly shows the widening of the initial modulation and a gain of 210 in bunching factor over the FEL section, which is sufficient for cooling.

Diffusion rate for CeC has been obtained using the final bunching factor shown in Figure 12, and parameters relevant to CeC experiment at BNL RHIC [16].

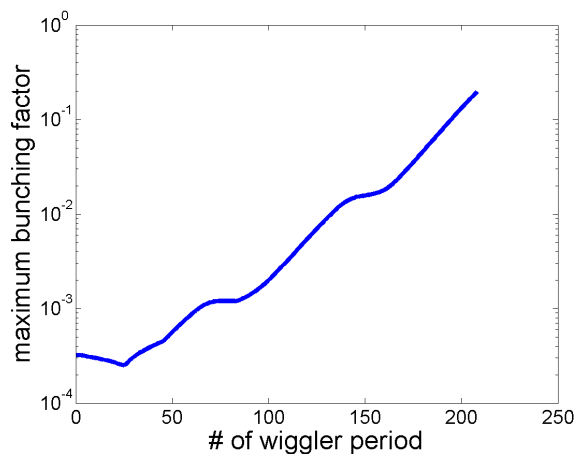


Figure 11: Evolution of bunching factor amplitude of shot noise in three-section FEL.

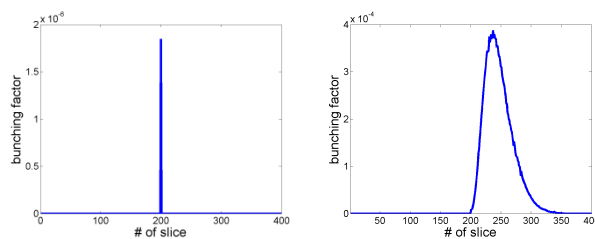


Figure 12: Bunching factor amplitude of modulation signal at the entrance (left) and exit (right) of FEL section.

### Kicker

In the kicker, ions interact with amplified modulation signals carried in electron beam and receive energy kick towards reference energy, which results in the cooling of ion beam. We take the output from GENESIS into SPACE for kicker simulations. Quadrupole setting in the kicker is symmetric with that in modulator. Electron beam envelope in the kicker is shown in Figure 13.

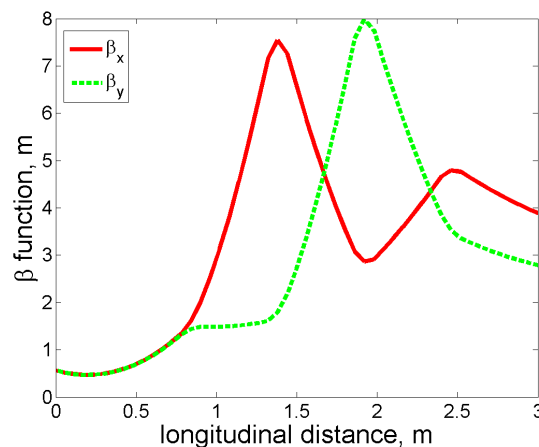


Figure 13: Evolution of electron beam  $\beta$  function in kicker section.

Figure 14 gives a close look at the amplified density modulation in the kicker section, and the coherent longitudinal velocity kick it gives to ions towards the reference energy. Red dot in Figure 14 represents ions

Content from this work may be used under the terms of the CC BY 3.0 licence (© 2018). Any distribution of this work must maintain attribution to the author(s), title of the work, publisher, and DOI.

with reference energy, and should receive zero energy kick. Green dots indicate ions with energy spread  $5.7e-4$  and this is the upper limit for CeC. Using ion beam with larger energy spread will result in inefficient cooling or even anti-cooling. Yellow dots are ions with energy spread  $3e-4$ , which is the value for CeC experiment listed in Table 1, and this is within the regime of efficient cooling.

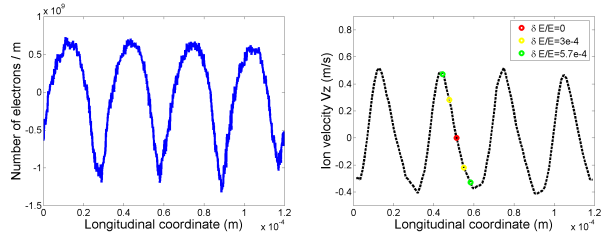


Figure 14: Amplified longitudinal density modulation in the kicker section (left) and the velocity kick it gives to ions at various longitudinal locations in a single pass through CeC system (right). Dots indicate specific ions with typical energy deviation.

We have traced ions with off-reference energies and the coherent kick they received in the kicker section, as is shown in Figure 15. As a result, we can predict the cooling time with only coherent kick included. A more realistic estimation of cooling time should include random kicks from surrounding ions and electrons.

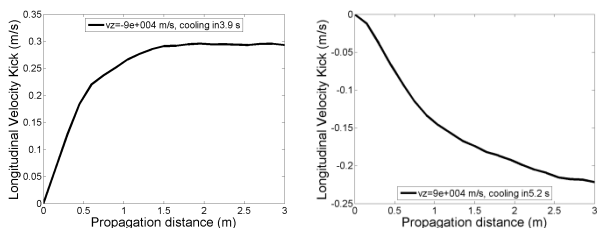


Figure 15: Coherent longitudinal velocity kick to a single ion with lower energy (left) and higher energy (right) with energy spread  $3e-4$  in the kicker section and cooling time. Values of velocities are in co-moving frame.

## SIMULATIONS OF PLASMA-CASCADE MICRO-BUNCHING AMPLIFIER

In the plasma-cascade micro-bunching amplifier, we have used strong solenoids to over-focus the electron beam and made use of the fast-growing plasma instability to boost the initial modulation, which acts as the amplifier for CeC. Designed parameters of PCA for RHIC and eRHIC at BNL are given in [4], and we present simulation studies of PCA using relevant settings.

Transverse beam size evolution in a four-cell PCA from numerical simulation is given in Figure 16. We have used very strong solenoid fields between cells to compress the beam and to make the plasma instability happen and grow. Figure 17 shows the gain we can get from the PCA. In Figure 17, we used Fast Fourier transform (FFT) to convert the longitudinal density distribution into frequency domain and calculate the gain in PCA section.

The maximum gain is about 120, which is sufficient for CeC, and it appears at around 30 THz.

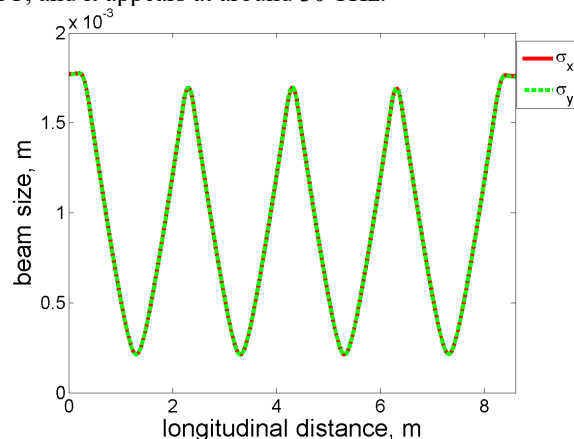


Figure 16: Evolution of transverse beam size in a four-cell plasma cascade amplifier.

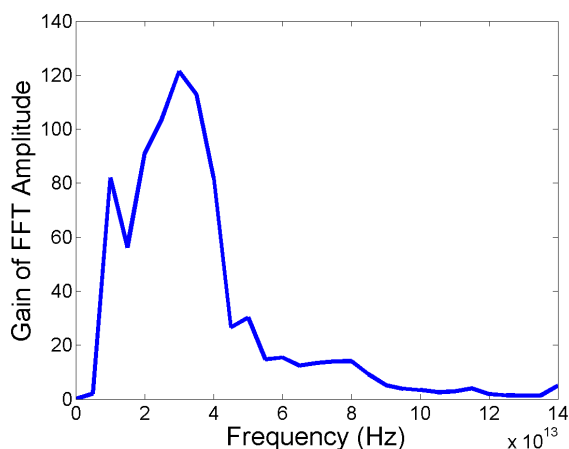


Figure 17: Gain of density modulation for various frequencies at the exit of PCA, calculated in frequency domain.

We have studied the evolution of signal over the PCA section by adding an initial modulation on top of the shot noise, and we have used the similar algorithm in modulator simulations to extract this signal from shot noise in PCA simulations. As is shown in Figure 18, we introduced an initial density modulation at 25 THz and observed the increase of the signal in PCA. Note that Figure 18 only presents the density modulation, and the sharp drops in Figure 18 indicate that density modulation has been transformed into velocity modulation.

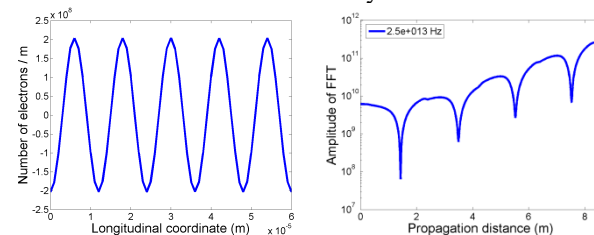


Figure 18: Initial density modulation (left) at the entrance of PCA and the amplification of density modulation (right) within the PCA section at frequency 25 THz.

Similarly, we added an initial velocity modulation to electron beam at the entrance of PCA at 25 THz and had the amplification in signal shown in Figure 19. Note that in the evolution plot of Figure 19, only density modulation is included. So the initial signal is small as we introduced pure velocity modulation, which has not converted into density modulation yet at the entrance of PCA.

A more realistic simulation will use a modulation signal induced by a real ion, which includes both density and velocity modulations and has a wider bandwidth instead of a specific frequency.

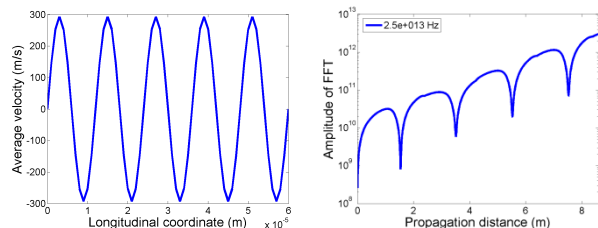


Figure 19: Initial velocity modulation (left) at the entrance of PCA and the amplification of density modulation (right) within the PCA section at frequency 25 THz.

Detailed beam dynamics in PCA section have been investigated, and we present the 2-D density distribution of modulation signal at several locations along the PCA beam line in Figure 20. Electrons at the transverse edge of the beam fall behind the central electrons, as they experience stronger solenoid focusing which introduces larger transverse motions to them and reduces their longitudinal velocities. An increase in density modulation is observed in Figure 20.

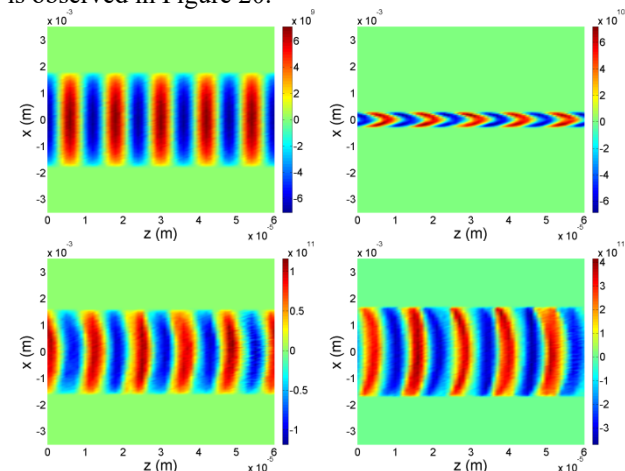


Figure 20: 2-D density modulation in the electron beam at the entrance of PCA (top left), middle of second cell (top right), end of third cell (bottom left) and exit of PCA (bottom right). X-axis is along the horizontal direction and z-axis is along the longitudinal direction.

We have quantified the delay of electrons at the beam edge compared with the central electrons, and present the result in Figure 21. The phase difference between central particle and edge particle is 45 degree, which is obtained from the fitting in Figure 21.

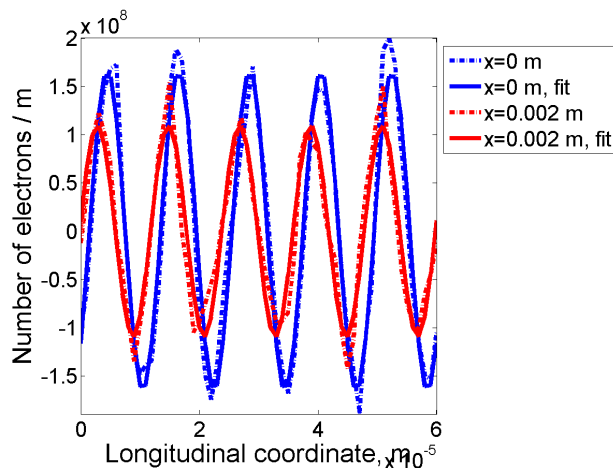


Figure 21: Comparison of density modulations between central electrons (blue lines) and electrons at transverse edge of the beam (red lines) at the exit of PCA.

## CONCLUSION

We present the simulation studies of CeC process using code SPACE and GENESIS.

We have successfully eliminated the shot noise and extracted the modulation signals in simulations using a single ion. Super position principle is justified in SPACE simulations. Simulation results have been verified through the comparison with analytical solutions to the modulator problem.

Start-to-end simulations have been performed for ions passing through the CeC system with FEL amplifier. We have studied the dependence of modulation process on various transverse offsets and off-reference energies of ions, and predicted the cooling time.

We have explored the use of plasma-cascade amplifier, which replaces the FEL amplifier in CeC. The gain and corresponding frequency in PCA have been obtained through numerical simulations. Detailed beam dynamics through the PCA have been analysed.

SPACE will be used in the further study of CeC to provide strong support to the design and operation of CeC experiment at BNL RHIC.

## REFERENCES

- [1] V. N. Litvinenko and Y. S. Derbenev, Free Electron Lasers and High-Energy Electron Cooling, in *Proc. FEL 2007*, Budker INP, Novosibirsk, Russia, BNL-79509-2007-CP.
- [2] V. N. Litvinenko, Coherent Electron Cooling, in *Proc. PAC 2009*, Vancouver, BC, Canada, paper FR1GRI01.
- [3] V.N. Litvinenko, Y.S. Derbenev, Coherent Electron Cooling, *Phys. Rev. Lett.* 102, 114801, 2009.
- [4] V. N. Litvinenko *et al.*, Plasma-Cascade Micro-Bunching Amplifier and Coherent Electron Cooling of A Hadron Beams, arXiv:1802.08677, 2018.
- [5] K. Yu *et al.*, Space Code for Beam-Plasma Interaction, in *Proc. IPAC 2015*, Richmond, VA, USA, MOPMN012.
- [6] K. Yu *et al.*, Simulation of Beam-Induced Plasma in Gas Filled Cavities, *Proc. IPAC 2015*, Richmond, VA, USA, paper MOPMN013.

- Content from this work may be used under the terms of the CC BY 3.0 licence (© 2018). Any distribution of this work must maintain attribution to the author(s), title of the work, publisher, and DOI.
- [7] J. Ma *et al.*, Simulation of Beam-Induced Plasma for the Mitigation of Beam-Beam Effects, in *Proc. IPAC 2015*, Richmond, VA, USA, paper MOPMN015.
- [8] X. Wang *et al.*, Adaptive Particle-in-Cloud method for optimal solutions to Vlasov-Poisson equation, *J. Comput. Phys.*, 316 (2016), 682-699.
- [9] S. Reiche, *Introduction on Genesis 1.3*, 2002, [http://genesis.web.psi.ch/download/documentation/gegenes\\_talk.pdf](http://genesis.web.psi.ch/download/documentation/gegenes_talk.pdf)
- [10] Y. Jing *et al.*, Model Independent Description of Amplification and Saturation Using Green's Function, arXiv:1505.04735, (2015).
- [11] G. Wang, M. Blaskiewicz, Dynamics of ion shielding in an anisotropic electron plasma, *Phys. Rev. E*, 78 (2008) 026413.
- [12] J. Ma *et al.*, Simulation Studies of Modulator for Coherent Electron Cooling, submitted to Physical Review Accelerators and Beams.
- [13] J. Ma *et al.*, Simulations of Modulator for Coherent Electron Cooling, *Proc. IPAC 2018*, Vancouver, BC, Canada, paper THPAF005.
- [14] J. Ma *et al.*, Modulator Simulations for Coherent Electron Cooling, *Proc. NAPAC 2016*, Chicago, IL, USA, paper WEPOA55.
- [15] J. Ma, Numerical Algorithms for Vlasov-Poisson Equation and Applications to Coherent Electron Cooling, Ph.D. Thesis, State University of New York at Stony Brook, ProQuest Dissertations Publishing, 2017.
- [16] J. Ma *et al.*, Simulation of Cooling Rate and Diffusion for Coherent Electron Cooling Experiment, *Proc. IPAC 2018*, Vancouver, BC, Canada, paper THPAF006.